Study of Restricted Diffusion in Porous Catalysts by NMR

The diffusion of 1,3,5 tri-tert-butylbenzene (TTB) into cylindrical γ-alumina extrudates of varying micropore diameter and macropore volume has been studied by NMR spectroscopy. The proton NMR signal of the methyl proton of TTB in the micropores of the alumina extrudate was found to be well resolved and shifted upfield relative to that in the bulk liquid by 0.55 ppm. The area under the shifted peak is proportional to the liquid concentration of TTB in the micropores. The change in the intensity of this peak as a function of time and measurements of the amount of TTB absorbed on the surface alumina at equilibrium were used to calculate the effective diffusivity of TTB in each extrudate. Measured values of the effective diffusivity are in reasonable agreement with predictions using correlations in the literature. These observations suggest a new method for measuring the liquid-phase effective diffusivity in porous materials.

W. C. Cheng
N. P. Luthra
C. J. Pereira
W. R. Grace & Co.-Conn.
Research Division
Columbia, MD 21044

Introduction

The effective diffusivity in porous catalysts is significantly reduced when the size of the molecule becomes comparable to the size of the pore due to configurational diffusion limitations (Andersen and Quinn, 1974). Spry and Sawyer (1975) proposed a fourth-power relationship between the effective diffusivity and 1 minus the ratio of the molecule size to the pore diameter. Chantong and Massoth (1983) have used model compound studies to verify this relationship.

Nuclear magnetic resonance (NMR) spectroscopy has been used extensively to characterize small pore crystalline materials such as zeolites (Thomas and Klinowski, 1985). Proton NMR has also been used to measure the diffusivity of hydrocarbons in zeolites (Karger and Pfeifer, 1987), hydrocarbon solvents in polymers (Fleischer, 1985), and hydrogen in metal hydrides (Mauger et al., 1981). The use of NMR for measuring effective diffusivity in γ-alumina extrudates has not been discussed in the literature.

The diffusion of 1,3,5 tri-tert-butylbenzene (TTB) in $CDCl_3$ solvent into cylindrical γ-alumina pellets of varying micropore diameter and macropore volume was studied using proton NMR. The proton NMR signal from the molecules in the pores was observed to be well resolved and shifted upfield relative to that of the molecules in the bulk liquid. This information and the results of separate equilibrium adsorption measurements were analyzed using a mathematical model to estimate effective diffusivity.

Experimental Method

Material

Commercially available SRA alumina (pseudoboehmite) from the Davison Chemical Division of W. R. Grace & Co. was used in the preparation of all the alumina extrudates. The unimodal samples (samples A–D) were prepared by peptizing the pseudoboehmite with an aqueous solution of nitric acid (HNO_3/Al_2O_3 molar ratio of 0.06) and extruding through a die containing circular openings of 3.2 mm dia. Samples of varying micropore diameter were prepared by calcining the extrudates at different temperatures. The bimodal extrudate (sample E) was prepared by adding a combustible organic material to the unpeptized alumina. Mercury penetration measurements were performed using Micromeritics Autopore 9200. The mercury intrusion curves shown in Figure 1 indicate that samples A–D are indeed unimodal, having no macropores (i.e., pores above 60 nm). Sample E has a similar surface area, micropore volume, and volume-averaged micropore diameter to sample B but contains substantial pore volume above 60 nm. The physical properties of these samples are summarized in Table 1.

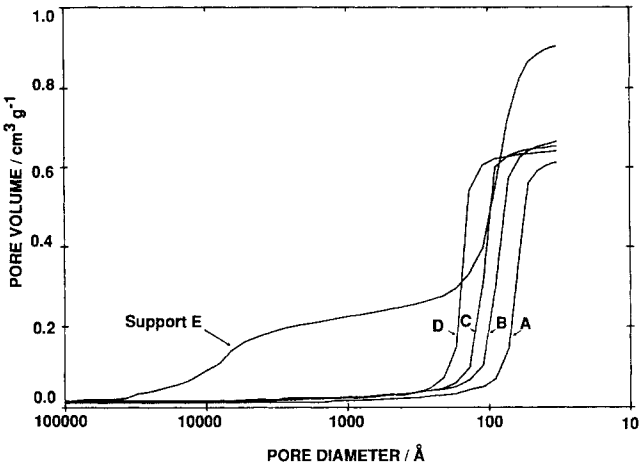

Figure 1. Pore size distributions by mercury porosimetry.

The TTB (97% purity) was obtained from Aldrich Chemical and deuterated chloroform was obtained from Merck, Sharp, and Dome. Both chemicals were used without further purification.

NMR procedure

The experiments were performed by placing a 3.2 cm long extrudate into a 5 mm NMR tube (4.17 mm ID), prefilling the pores of the extrudate with $CDCl_3$, adding a solution containing 4.07×10^{-5} mol/cm^3 TTB in $CDCl_3$ into the NMR tube so that the liquid just covered the top of the extrudate, and placing the probe in the NMR instrument. The time elapsed between injecting the liquid to the start of data collection was approximately 1 min. Since the annular space between the extrudate and the NMR tube was only 0.8 mm, the solution external to the extrudate was assumed to be well mixed. Furthermore, the concentration of TTB was assumed to be axially uniform.

Time-dependent proton NMR spectra were obtained in the Fourier transform mode on a Bruker AM-400 superconducting spectrometer (400.13 MHz). Measurements were made at 295 ± 1 K using $CDCl_3$ as an internal lock solvent. Chemical shifts were measured with respect to Me_4Si and are accurate to ±0.002 ppm.

Equilibrium adsorption measurements

Adsorption of the solute on the alumina surface could affect the rate of diffusion (Satterfield et al., 1973). In order to take this effect into account the equilibrium adsorption kinetics of TTB on γ-alumina were measured. This was done by placing 0.8 mm γ-alumina extrudates (presoaked in $CDCl_3$) in solutions of varying TTB content. Four grams of alumina having a surface area of 263 m^2/g and approximately 10 cm^3 of solution were used in each experiment. The disappearance of TTB from solution at equilibrium was measured by UV absorbance using a Gilford Response UV instrument. The uptake on the solid was obtained from the difference between the initial and final concentration of TTB in the solution.

Data Analysis

Using the equilibrium adsorption measurements, adsorption of TTB on the alumina surface was determined to follow Langmuir kinetics:

$$s = \frac{Ks_{sat}c}{(1 + Kc)} \tag{1}$$

where s is the concentration of TTB adsorbed on the solid, s_{sat} is the saturation concentration on the solid, c is the concentration of TTB in the solution, and K is the equilibrium constant. A plot of $1/s$ v. $1/c$ is shown in Figure 2. Values of $K = 1.9 \times 10^6$ cm^3/mol and $s_{sat} = 8.3 \times 10^{-12}$ mol/cm^2 were obtained from the slope and intercept of the least square fit line in Figure 2. For a 10.3 Å diameter TTB molecule, the s_{sat} value corresponds to a low surface coverage of approximately 5%. The low coverage is due to the nonpolar nature of TTB and the bulky t-butyl groups that inhibit ordered packing. The large value of K suggests that $s \approx s_{sat}$, and that the TTB on the solid moves as a sharp front into the extrudate.

The isothermal mass conservation equation for the diffusion of TTB into the extrudate is:

$$\left\{\epsilon_t + \frac{s_g \rho_p K s_{sat}}{(1 + Kc_o u)} \frac{\partial u}{\partial \tau}\right\} = \frac{1}{\xi} \frac{\partial}{\partial \xi}\left[\xi \frac{\partial u}{\partial \xi}\right] \tag{2}$$

with boundary conditions

$$u(1, \tau) = v \tag{3a}$$

$$\frac{\partial u}{\partial \xi}(0, \tau) = 0 \tag{3b}$$

Table 1. Physical Properties of γ-alumina Extrudates

	Sample				
	A	B	C	D	E
Extrudate dia., cm	0.262	0.260	0.258	0.250	0.271
Hg pore volume, cm^3/g	0.612	0.665	0.653	0.641	0.904
Macropore vol. (>60 nm)	0.021	0.032	0.027	0.031	0.243
Micropore vol. (<60 nm)	0.591	0.633	0.626	0.610	0.661
Surface area, m^2/g*	363 (253)	304 (201)	239 (167)	172 (113)	318 (285)
Extrudate density, g/cm^3	1.057	1.038	1.052	1.071	0.806
Extrudate void frac., cm^3/cm^3	0.647	0.690	0.687	0.687	0.729
Micropore dia., nm**	6.6 (9.3)	8.2 (12.6)	10.0 (15.0)	16.0 (21.6)	8.3 (9.3)

*Numbers in parentheses are BET surface areas
**Numbers in parentheses calculated as 4 × micropore volume/BET area

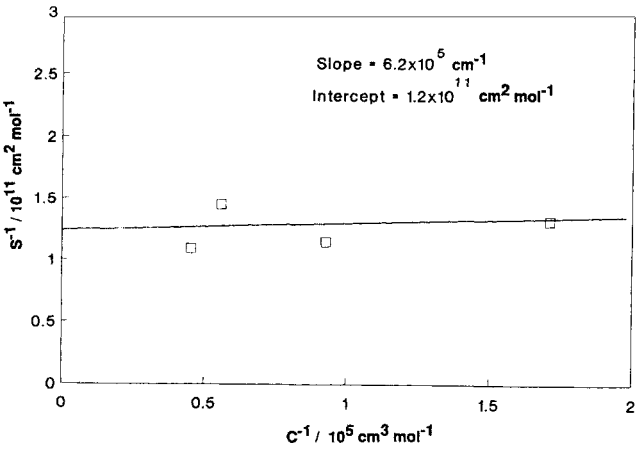

Figure 2. Plot of $1/s$ vs. $1/c$ from equilibrium adsorption experiments.

and the initial condition

$$u(\xi, 0) = 0 \tag{4}$$

u is the dimensionless concentration in the extrudate, ξ is the fractional distance from the center of the extrudate, τ is the dimensionless time, c_o is the initial concentration outside the extrudate, v is the dimensionless concentration outside the extrudate, ϵ_t is the total porosity, s_g is the surface area, ρ_p is the extrudate density. The dimensionless time, τ, is defined as $D_e t/R^2$ where D_e is the effective diffusivity, t is the time, and R is the radius of the pellet. Equation 2 implies that local adsorption equilibrium is established very much faster than the time of diffusion into the extrudate.

The mass conservation equation for TTB in the solution outside the extrudate is

$$\frac{dv}{d\tau} = -\alpha \left.\frac{\partial u}{\partial \xi}\right|_{\xi = 1} \tag{5}$$

with initial condition

$$v(0) = 1 \tag{6}$$

where α is the ratio of the extrudate volume to the volume of the external solution. The mass conservation equation for TTB may be used to replace Eq. 5 and 6. The concentration in the external liquid is:

$$v = 1 - 2\alpha \int_0^1 \left[\epsilon_t u + \frac{s_g \rho_p K s_{sat} u}{(1 + K c_o u)}\right] \xi \, \partial\xi \tag{7}$$

The ratio of the moles of TTB in the micropores of the extrudate to the moles of TTB outside the extrudate, $\Psi(\tau)$, is:

$$\Psi = \frac{2\alpha\epsilon_{\text{mic}}}{v} \int_0^1 u\xi \, d\xi \tag{8}$$

Equations 1 to 4 and 7 are solved using a finite-difference scheme to obtain $u(\xi, \tau)$ and $v(\tau)$. Equation 8 is then used to calculate $\Psi(\tau)$.

Since $s \approx s_{sat}$, the shell penetration model (SPM) may be used to estimate Ψ and the position of the TTB front in the solid (ξ_{SPM}) with time. The SPM assumes that the diffusion in the outer shell (in which the solid concentration is s_{sat}) is at pseudosteady state. The concentration outside the extrudate using SPM is:

$$v_{SPM} = \frac{[1 - \alpha s_g \rho_p s_{sat}(1 - \xi_{\text{SPM}}^2)/c_o]}{\{1 + \epsilon_t \alpha [1 + (1 - \xi_{SPM}^2)/2 \ln \xi_{SPM}]\}} \tag{9}$$

where ξ_{SPM} is the location of the front. The relationship between ξ_{SPM} and τ is obtained by solving the implicit equation:

$$\tau = \int_1^{\xi SPM} [s_g \rho_p s_{\text{sat}} \ln \xi / v(\xi)] \, \xi d\xi \tag{10}$$

The ratio of moles of TTB inside the micropores of the extrudate to moles in the external liquid is:

$$\Psi_{\text{SPM}} = \epsilon_{\text{mic}} \alpha [1 + (1 - \xi_{SPM}^2)/2 \ln \xi_{SPM}] \tag{11}$$

Using Eq. 9 to 11, for a given value of ξ_{SPM} both τ and Ψ_{SPM} can be calculated.

Results and Discussion

Typical proton NMR spectrum of a TTB solution in contact with γ-alumina is shown in Figure 3. Both the peaks of the aromatic protons and the methyl protons are shifted upfield relative to that of the molecule in the bulk liquid by about 0.55 ppm.

The proton NMR spectra of the methyl protons of TTB in $CDCl_3$ solvent at varying times of contact with the cylindrical alumina extrudate are shown in Figure 4. The area under the proton NMR signal from the molecules in the pores increases with time. Figure 4 also shows that the NMR signal of TTB in the micropores is broader than that in the bulk liquid. The line broadening of the peaks is due to two factors, the hindrance to molecular rotation within the pores (Boddenberg and Burmeister, 1988) and the exchange between molecules in the liquid phase and the physisorbed molecules. Figure 5 shows that the line width of both the aromatic and the methyl protons of TTB

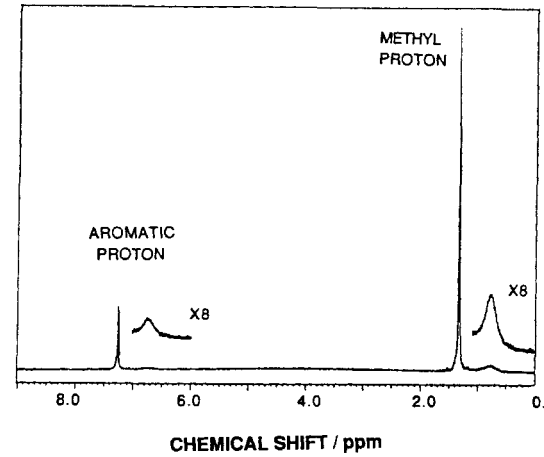

Figure 3. Proton NMR spectrum of tri-tert-butylbenzene in contact with alumina.

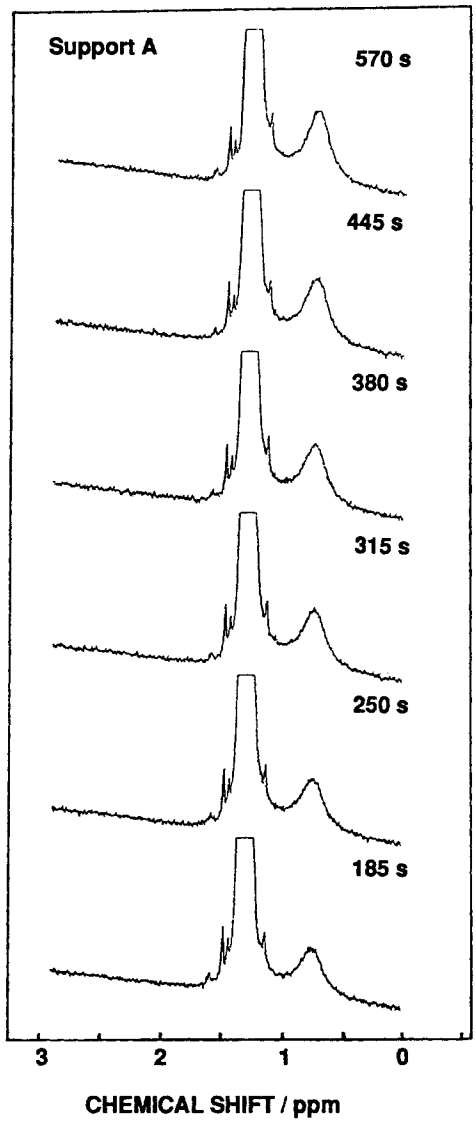

Figure 4. Proton NMR spectra of tri-tert-butylbenzene diffusing into the pores of alumina.
Spinning side bands at 1.1, 1.4, and 1.5 ppm

increases as the ratio of the molecule size to the micropore diameter increases. The increased pore diameter allows for freer rotation and the decreased surface area leads to less physisorption. Above a diameter of 100Å, the line width becomes constant. This shows that the interaction between TTB and the support becomes constant at a pore diameter of 100Å.

The ratio of the area under the proton NMR signal from molecules in the pores to the area from molecules in the bulk liquid, Ψ, increases with time, as shown in Figure 6. The rate of increase of Ψ is a measure of the diffusion rate. As shown in Figure 6, the rate of diffusion of TTB increases with the average micropore diameter of unimodal extrudates and increases (for a given micropore diameter) with increasing macropore volume. If the area under the proton NMR signal in the pores represents the moles of TTB in the micropores, then Ψ should approach the ratio of the micropore volume in the alumina extrudate to the external liquid volume after a very long time. The final values of Ψ, taken after 18 h, were found to be about 20% lower than the

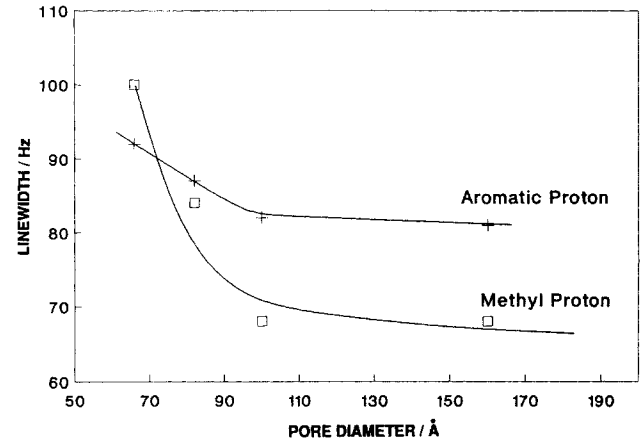

Figure 5. Line width in NMR signal as a function of pore diameter.

ratio of the micropore volume to the exterior volume. This lower experimental Ψ value is attributed to structural interference (Fraissard and Ito, 1988). In our calculations, Ψ was taken as the ratio of the moles of TTB in the micropores to the moles of TTB in the bulk liquid.

An estimate of how far TTB penetrates into the extrudate during the course of the experiments is obtained from the SPM. For various values of ξ_{SPM}, Ψ_{SPM} is obtained using Eq. 11. As shown in Table 2, ξ_{SPM} values of between 0.59 and 0.77 are estimated when the first observation is made. A larger molecule or a more viscous solvent could be used to obtain spectra earlier on in the diffusion process.

The effective diffusivity for each extrudate is determined as follows. Equations 2 to 4 and 7 are solved using a finite-difference algorithm. In our calculations, the ξ dimension was discretized into 101 grid points with τ steps of 1×10^{-4}. Equation 8 was used to calculate Ψ as a function of τ. Next, a value of τ was determined for each experimental Ψ value. Plots of τ vs. time for each extrudate are shown in Figure 7. The values of the effective diffusivity, obtained by multiplying the slope of these lines by the square of the radius of each extrudate, are shown in Table 2. Also shown in Table 2 are effective diffusivities calculated using the SPM. Due to the assumptions

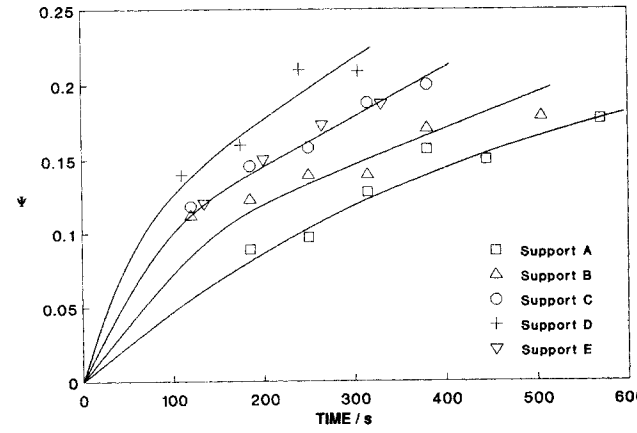

Figure 6. Ratio of moles of TTB inside extrudate to moles TTB in external solution v. time.

Table 2. Effective Diffusivity of TTB in Cylindrical Alumina Extrudates

Sample	ϵ_{mic}	ϵ_{mac}	λ	SPM Results		$De \times 10^6$, cm^2/s	
				ξ_{SPM} Range	$D_{e,SPM} \times 10^6$	Calc.	Pred.
A	0.625	0.022	0.156	(0.77, 0.40)	2.74	3.22	3.93
B	0.657	0.033	0.126	(0.72, 0.54)	2.96	3.93	4.84
C	0.658	0.028	0.103	(0.70, 0.46)	3.61	5.33	5.27
D	0.653	0.033	0.064	(0.59, 0.36)	4.22	7.44	6.19
E	0.533	0.196	0.124	(0.67, 0.47)	4.85	6.91	5.91

of the SPM, these diffusivities represent a lower bound on the value of the effective diffusivity.

The ratio of the molecule size to the volume-averaged micropore diameter obtained from mercury porosimetry, λ, for each extrudate is also shown in Table 2. For unimodal extrudates, the effective diffusivity decreases with increasing λ. For similar values of λ, effective diffusivity increases with increasing macroporosity.

The bulk diffusivity, D_b, was estimated to be between 1.24×10^{-5} using the Scheibel correlation and 1.81×10^{-5} cm^2/s using the Wilke-Chang correlation (Reid et al., 1977). Effective diffusivities were predicted using a D_b/TOR value of 1.16×10^{-5} cm^2/s in the equation:

$$D_e = \frac{D_b}{TOR}\left[\epsilon_{mac} + \epsilon_{mic}(1-\lambda)^4\right] \tag{12}$$

where TOR is the tortuosity. For the D_b values estimated above, TOR values range between 1.07 and 1.56. D_e values predicted using Eq. 12 are shown in Table 2. There is reasonable agreement between calculated and predicted D_e values. For the unimodal catalysts, calculated D_e values were found to follow a power greater than 4. Possible explanations for this could be the fact that there are only four data points. Scatter in the estimation of D_e within a limited set of experiments has been observed in the literature (Chantong and Massoth, 1983). Equation 12 was unable to represent the trend in D_e when micropore diameters using BET surface areas were used.

The reciporcal line width of the proton NMR signal in the micropores is plotted vs. λ in Figure 8. The reciprocal line width is constant for $\lambda < 0.1$ but decreases for $\lambda > 0.1$. Since the reciprocal line width is a measure of rotational mobility, the results indicate that on the NMR time scale, the TTB molecules become free to rotate at $\lambda < 0.1$. However, the effective diffusivity, which is related to the translational mobility, increases monotonically as λ decreases from 0.156 to 0.064.

Conclusions

A new method of measuring the liquid-phase effective diffusivity of molecules in porous materials has been developed. The method, based on proton NMR, has been used to study the diffusion of tri-tert-butylbenzene in γ-alumina extrudates of varying pore structure. Values of effective diffusivity calculated using a diffusion-adsorption model are in good agreement with the predictions using correlations in the literature. Additionally, line broadening of the proton NMR signal increases with decreasing pore diameter and gives a good measure of configurational restriction to diffusion.

Notation

c = concentration, mol/cm^3
D = diffusivity
K = equilibrium constant, cm^3/mol
R = radius of extrudate, cm
s = solid concentration, mol/cm^2
s_g = surface area, cm^2/g
t = time, s
TOR = tortuosity
u = dimensionless concentration in the extrudate
v = dimensionless concentration outside the extrudate

Greek letters

α = ratio of extrudate volume to external liquid volume

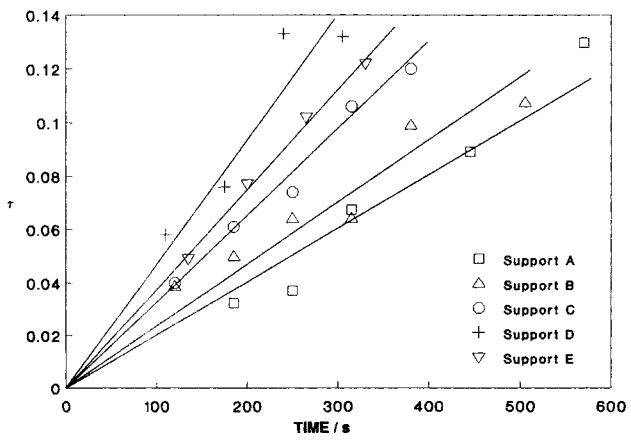

Figure 7. τ vs. time for each extrudate.
Slope of solid line is D_e/R^2

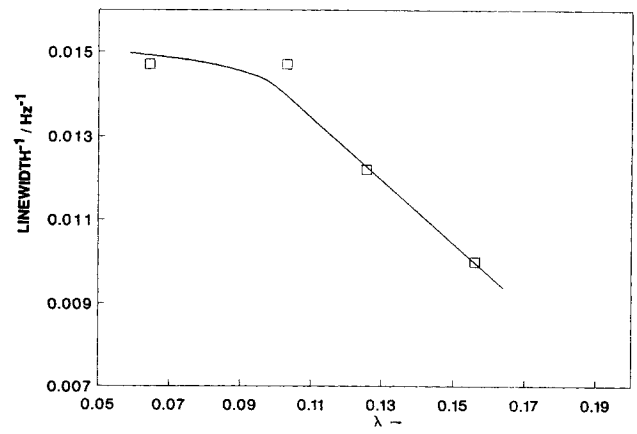

Figure 8. Inverse line width vs. ratio of molecule diameter to micropore diameter for unimodal extrudate samples A–D.

λ = ratio of molecule size to micropore diameter
ϵ = porosity
ρ_p = extrudate density, g/cm^3
ξ = fractional distance from center of extrudate
τ = dimensionless time, $D_e t / R^2$
Ψ = ratio of moles in micropores to moles in bulk liquid

Subscripts

b = bulk value
e = effective
o = initial value
mac = macropore
mic = micropore
sat = saturation concentration
t = total
SPM = shell progressive model

Literature Cited

Andersen, J. L., and J. A. Quinn, "Restricted Transport in Small Pores. A Model for Steric Exclusion and Hindered Particle Motion." *Biophysical J.*, **14,** 130 (1974).

Boddenberg, B., and Burmeister, R., "^{2}H NMR Study on the Rotation and Diffusion Kinetics of Propene and Benzene in NaX and AgNaX Zeolites," *Zeolites,* **8,** 488 (1988).

Chantong, A., and F. E. Massoth, "Restrictive Diffusion in Aluminas," *AIChE J.*, **29,** 725 (1983).

Fleischer, G., "Studies of Diffusion of Benzene-Cyclohexane and Benzene-Toluene Mixtures in Polyethylene using Pulsed Field Gradient NMR Technique," *Polymer Comm.*, **26,** 20 (1985).

Fraissard, J., and T. Ito, "^{129}Xe NMR Study of Adsorbed Xenon: A New Method for Studying Zeolites and Metal-zeolites," *Zeolites,* **8,** 350 (1988).

Karger, J., and H. Pfeifer, "NMR Self-diffusion Studies in Zeolite Science and Technology," *Zeolites,* **7,** 90 (1987).

Mauger, P. E., W. D. Williams, and R. M. Cotts, "Diffusion and NMR Spin Lattice Relaxation of ^{1}H in $\ddot{\alpha}^1$ TaH_x and NbH_x," *J. Phys. Chem. Solids,* **42,** 821 (1981).

Reid, R. C., J. M. Prausnitz, and T. K. Sherwood, *The Properties of Gases and Liquids,* McGraw-Hill, New York (1977).

Thomas, J. M., and J. Klinowski, "The Study of Aluminosilicate and Related Catalysts by High-resolution Solid-state NMR Spectroscopy," *Adv. Catal.*, **33,** 199 (1985).

Satterfield, C. N., C. K. Colton, and W. H. Pitcher, Jr., "Restricted Diffusion in Liquids within Fine Pores," *AIChE J.*, **19,** 628 (1973).

Spry, J. C., and W. H. Sawyer, "Configurational Diffusion Effects in Catalytic Demetallization of Petroleum Feedstocks," AIChE Nat. Meet., Los Angeles (1975).

Manuscript received July 25, 1989, and revision received Feb. 1, 1990.